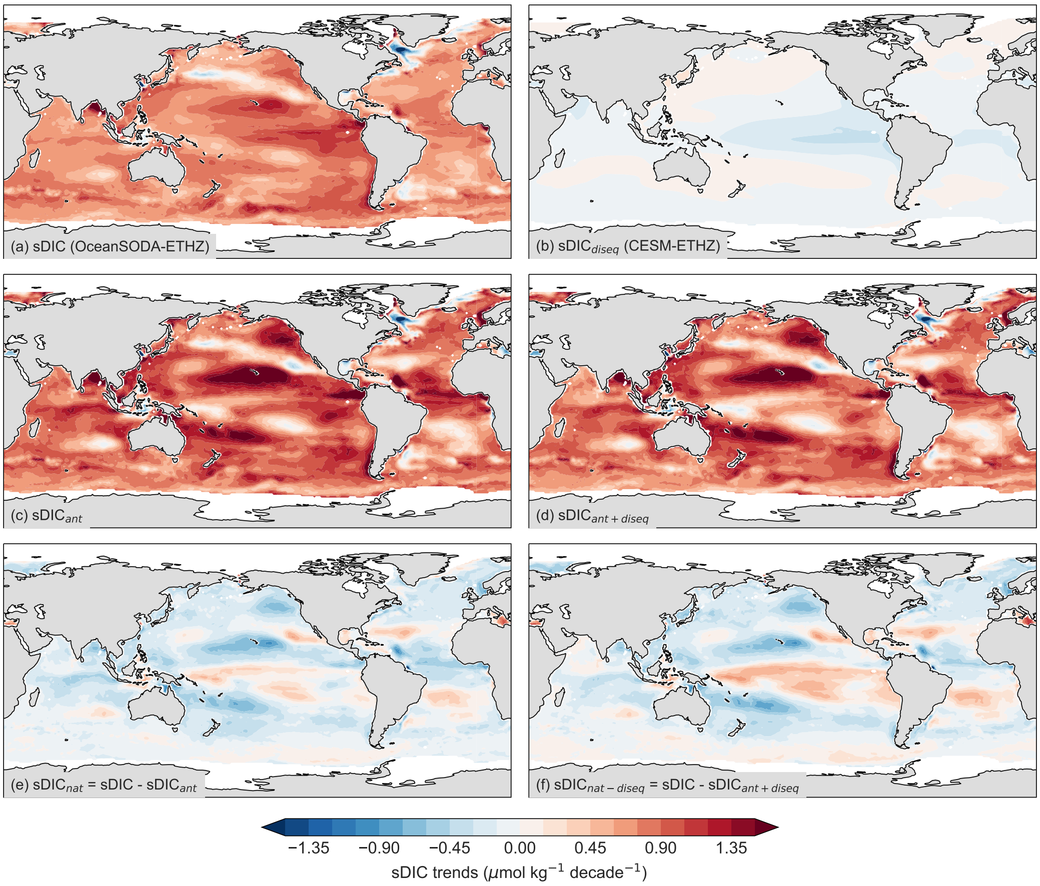

Figure S1. Maps of the slopes of salinity normalized DIC (sDIC) for various components. (a) sDIC trends from OceanSODA-ETHZ (Gregor & Gruber, 2021). (b) The disequilibrium term was calculated as the difference between oceanic and atmospheric pCO_2 for a CESM-ETHZ model run with increasing CO_2 and constant climate (run C). The pCO_2 disequilibrium was added to OceanSODA-ETHZ pCO_2 from which DIC was calculated with *PyCO2SYS*. (c) The expected increase in sDIC if pCO_2 followed atmospheric pCO_2 perfectly. (d) The increase in sDIC when accounting for the disequilibrium where uptake slows due to natural outgassing. (e) The slope of the natural sDIC component is calculated as the residual of (a) - (c). (f) The slope of the natural sDIC component including the disequilibrium term calculated as (a) - (d).

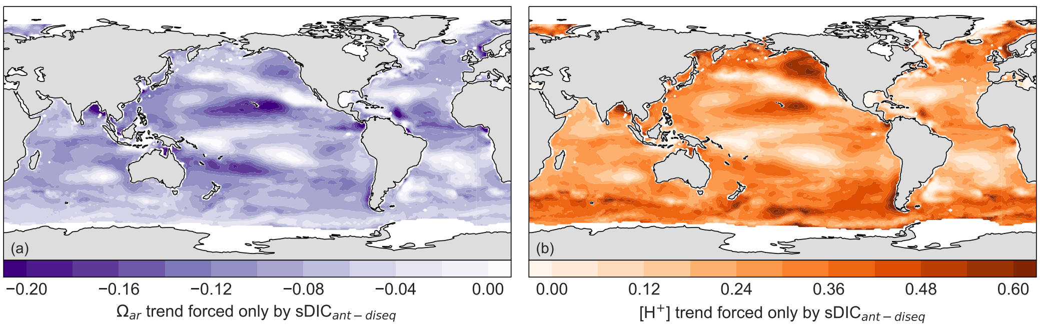

Figure S2. Expected increases in (a) Ω_{ar} and (b) $[H^+]$ due to an increase in sDIC$_{ant+diseq}$ (shown in Figure S1d).

Table S1. Trends for pH and Ω_{ar} (units per decade) from various sources in the literature compared with OceanSODA-ETHZ for the same periods. Note that these trends may not compare well with OceanSODA-ETHZ results due to the different methods used to calculate the trends.

			pH (decade^{-1})		Ω_{ar} (decade^{-1})		
Station	Location	Period	Trend	Literature	Trend	Literature	Reference
BATS	32.0°N, 64.0°W	1983-2012	-0.014 ± 0.000	-0.017 ± 0.001	-0.066 ± 0.006	-0.095 ± 0.007	(Bates et al., 2014)
		1983-2020	-0.016 ± 0.000	-0.019 ± 0.001	-0.060 ± 0.004	-0.090 ± 0.010	(Bates & Johnson, 2020)
HOT	22.8°N, 158.0°W	1988-2007	-0.014 ± 0.001	-0.019 ± 0.002	-0.095 ± 0.013		(Dore et al., 2009)
		1988-2012	-0.015 ± 0.001	-0.016 ± 0.001	-0.098 ± 0.009	-0.084 ± 0.011	(Bates et al., 2014)
ESTOC	29.0°N, 15.5°W	1995-2012	-0.016 ± 0.001	-0.018 ± 0.002	-0.072 ± 0.014	-0.115 ± 0.023	(Bates et al., 2014)
Iceland Sea	68.0°N, 12.7°W	1983-2012	-0.019 ± 0.001	-0.014 ± 0.005	-0.056 ± 0.006	-0.018 ± 0.027	(Bates et al., 2014)
Irminger Sea	64.3°N, 28.0°W	1983-2012	-0.018 ± 0.000	-0.026 ± 0.006	-0.046 ± 0.007	-0.080 ± 0.040	(Bates et al., 2014)
Munida	45.7°S, 171.5°E	1998-2012	-0.019 ± 0.001	-0.013 ± 0.003	-0.122 ± 0.024	-0.085 ± 0.026	(Bates et al., 2014)
CARIACO	10.5°N, 64.7°W	1995-2012		-0.025 ± 0.004		-0.066 ± 0.028	(Bates et al., 2014)
137°E tropics	5-10°N, 137.0°E	1983-2017	-0.013 ± 0.000	-0.012 ± 0.008	-0.065 ± 0.005	-0.081 ± 0.050	(Ono et al., 2019)
137°E subtropics	20-22°N, 137.0°E	1983-2017	-0.016 ± 0.000	-0.017 ± 0.007	-0.080 ± 0.005	-0.113 ± 0.040	(Ono et al., 2019)
137°E Kuriosho	26-30°N, 137.0°E	1983-2017	-0.017 ± 0.001	-0.019 ± 0.008	-0.090 ± 0.006	-0.121 ± 0.050	(Ono et al., 2019)

Table S2. Comparison of trends (units per decade) for long-term observation stations. pH and Ω_{ar} were calculated from DIC and Alk for the observation stations and OceanSODA-ETHZ was calculated from pCO_2 and Alk. Uncertainties are the standard error associated with the slope coefficient and do not include other uncertainties associated with measurements or predictions.

			pH		Ω_{ar}	
Station	Location	Period	Observations	OS-ETHZ	Observations	OS-ETHZ
BATS	31.5°N, 64.5°W	1992-2021	-0.0166 ± 0.001	-0.0174 ± 0.000	-0.0625 ± 0.010	-0.0605 ± 0.005
HOT	22.5°N, 158.5°W	1989-2021	-0.0180 ± 0.001	-0.0182 ± 0.001	-0.0888 ± 0.006	-0.0826 ± 0.005
ESTOC	29.5°N, 15.5°W	1995-2009	-0.0139 ± 0.003	-0.0155 ± 0.001	-0.1375 ± 0.013	-0.0676 ± 0.020

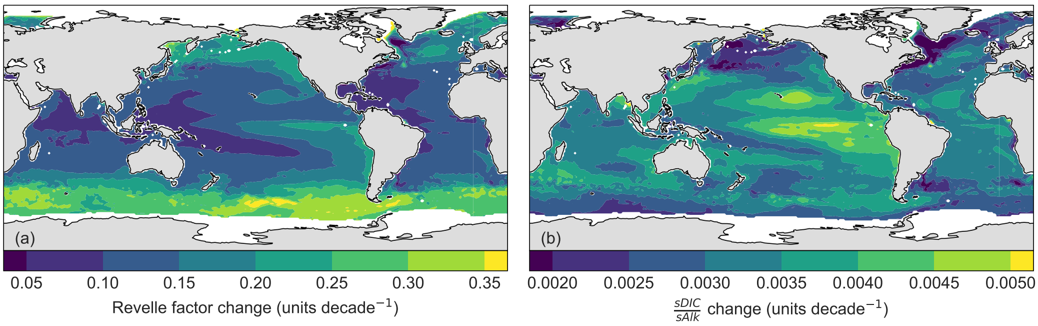

Figure S3. (a) Map showing the rates of Revelle factor change and (b) map showing the rates of DIC/Alk ratio change.

Table S3. Slopes of Ω_{ar} (units per decade) decomposed into mechanisms (Mech.) for each driver. The regions are biomes from (Fay & McKinley, 2014), where the ice-covered biomes are not presented. We decompose sDIC into anthropogenic (sDIC^{ant}) and natural (sDIC^{nat}) components, where the latter is the residual of sDIC minus the anthropogenic component. We also show the actual trend for the variable (Trend) and the sum of the decomposed components (Σ). The mechanisms are taken from Eq 2., where m.e. indicates the mass effect.

Region	Trend	Σ	Mech.	sDIC^{ant}	sDIC^{nat}	sDIC	sAlk	Temp	FW
GLOBAL	-0.0711	-0.0712	ΔX	-0.0869	0.0158	-0.0711	-0.0051	0.0028	0.0020
			ω_X	-0.0039	0.0005	-0.0034	0.0000	-0.0000	-0.0000
			Ω_{ar} m.e.	0.0044	-0.0006	0.0038	-0.0001	-0.0001	0.0000
NP-SPSS	-0.0479	-0.0491	ΔX	-0.0736	0.0269	-0.0467	-0.0054	0.0022	0.0005
			ω_X	-0.0025	0.0005	-0.0019	-0.0003	-0.0000	-0.0000
			Ω_{ar} m.e.	0.0032	-0.0008	0.0024	0.0002	-0.0001	-0.0000
NP-STSS	-0.0689	-0.0697	ΔX	-0.0844	0.0243	-0.0601	-0.0167	0.0040	0.0032
			ω_X	-0.0028	0.0006	-0.0022	-0.0012	-0.0000	-0.0000
			Ω_{ar} m.e.	0.0031	-0.0007	0.0024	0.0012	-0.0001	-0.0002
NP-STPS	-0.0809	-0.0818	ΔX	-0.1074	0.0272	-0.0801	-0.0055	0.0036	0.0003
			ω_X	-0.0033	0.0003	-0.0030	-0.0007	-0.0000	-0.0000
			Ω_{ar} m.e.	0.0035	-0.0004	0.0032	0.0007	-0.0001	-0.0002
PEQU-W	-0.0647	-0.0652	ΔX	-0.0740	0.0092	-0.0648	-0.0115	0.0045	0.0069
			ω_X	-0.0035	0.0006	-0.0029	0.0000	-0.0000	-0.0000
			Ω_{ar} m.e.	0.0033	-0.0006	0.0027	-0.0000	-0.0001	-0.0000
PEQU-E	-0.0981	-0.0975	ΔX	-0.1074	0.0019	-0.1055	0.0079	0.0012	-0.0024
			ω_X	-0.0038	-0.0035	-0.0073	-0.0002	0.0000	-0.0000
			Ω_{ar} m.e.	0.0045	0.0038	0.0083	0.0002	0.0004	-0.0001
SP-STPS	-0.0795	-0.0796	ΔX	-0.0978	0.0180	-0.0798	-0.0039	0.0026	0.0014
			ω_X	-0.0038	0.0003	-0.0035	-0.0002	-0.0000	-0.0000
			Ω_{ar} m.e.	0.0042	-0.0004	0.0038	0.0002	-0.0001	-0.0001
NA-SPSS	-0.0452	-0.0457	ΔX	-0.0635	0.0261	-0.0374	-0.0139	0.0032	0.0023
			ω_X	-0.0027	0.0008	-0.0019	-0.0002	-0.0000	-0.0000
			Ω_{ar} m.e.	0.0034	-0.0010	0.0024	-0.0001	-0.0001	-0.0000
NA-STSS	-0.065	-0.0652	ΔX	-0.0873	0.0229	-0.0644	-0.0078	0.0037	0.0035
			ω_X	-0.0033	0.0009	-0.0024	-0.0002	-0.0000	-0.0000
			Ω_{ar} m.e.	0.0034	-0.0009	0.0025	0.0002	-0.0002	-0.0001
NA-STPS	-0.0676	-0.0673	ΔX	-0.0842	0.0103	-0.0739	-0.0033	0.0044	0.0057
			ω_X	-0.0034	0.0007	-0.0027	0.0000	-0.0000	-0.0000
			Ω_{ar} m.e.	0.0034	-0.0007	0.0027	-0.0000	-0.0001	-0.0001
AEQU	-0.0774	-0.0783	ΔX	-0.1254	0.0393	-0.0862	0.0074	0.0039	-0.0036
			ω_X	-0.0055	0.0023	-0.0032	0.0006	-0.0000	-0.0000
			Ω_{ar} m.e.	0.0059	-0.0024	0.0034	-0.0007	-0.0002	0.0003
SA-STPS	-0.0719	-0.071	ΔX	-0.0621	-0.0018	-0.0640	-0.0172	0.0025	0.0076
			ω_X	-0.0049	0.0015	-0.0034	0.0003	-0.0000	0.0000
			Ω_{ar} m.e.	0.0049	-0.0015	0.0034	-0.0003	-0.0001	0.0002
IND-STPS	-0.0734	-0.0737	ΔX	-0.0940	0.0205	-0.0735	-0.0064	0.0035	0.0026
			ω_X	-0.0047	0.0013	-0.0033	0.0002	-0.0000	0.0000
			Ω_{ar} m.e.	0.0048	-0.0013	0.0034	-0.0002	-0.0001	0.0001
SO-STSS	-0.0667	-0.0664	ΔX	-0.0771	0.0155	-0.0616	-0.0095	0.0021	0.0021
			ω_X	-0.0047	0.0008	-0.0039	0.0004	-0.0000	-0.0000
			Ω_{ar} m.e.	0.0055	-0.0009	0.0046	-0.0006	-0.0001	0.0001
SO-SPSS	-0.0616	-0.0605	ΔX	-0.0707	0.0033	-0.0674	0.0058	0.0004	-0.0006
			ω_X	-0.0041	0.0002	-0.0040	0.0008	-0.0000	-0.0000
			Ω_{ar} m.e.	0.0058	-0.0002	0.0055	-0.0011	-0.0000	0.0001

Table S4. The same as Table S3 but for $[H^+]$ in $nmol \cdot kg^{-1} \cdot decade^{-1}$.

Region	Trend	Σ	Mech.	sDIC^{ant}	sDIC^{nat}	sDIC	sAlk	Temp	FW
GLOBAL	0.2502	0.2853	ΔX	0.2510	-0.0438	0.2073	0.0106	0.0381	0.0037
			β_X	0.0083	-0.0010	0.0073	-0.0003	-0.0000	-0.0000
			$[H^+]$ m.e.	0.0195	-0.0025	0.0170	-0.0003	0.0019	0.0000
NP-SPSS	0.2777	0.314	ΔX	0.3274	-0.1165	0.2109	0.0171	0.0561	0.0012
			β_X	0.0085	-0.0020	0.0066	0.0009	-0.0000	-0.0001
			$[H^+]$ m.e.	0.0201	-0.0045	0.0156	0.0021	0.0033	0.0003
NP-STSS	0.2575	0.3006	ΔX	0.2333	-0.0695	0.1638	0.0418	0.0601	0.0071
			β_X	0.0054	-0.0012	0.0042	0.0026	-0.0000	-0.0001
			$[H^+]$ m.e.	0.0130	-0.0026	0.0104	0.0061	0.0036	0.0010
NP-STPS	0.2392	0.274	ΔX	0.2543	-0.0634	0.1910	0.0135	0.0449	0.0011
			β_X	0.0050	-0.0004	0.0045	0.0013	-0.0000	-0.0001
			$[H^+]$ m.e.	0.0126	-0.0011	0.0115	0.0029	0.0026	0.0008
PEQU-W	0.2124	0.2477	ΔX	0.1673	-0.0208	0.1464	0.0217	0.0512	0.0114
			β_X	0.0049	-0.0008	0.0040	-0.0000	-0.0000	-0.0001
			$[H^+]$ m.e.	0.0145	-0.0026	0.0119	-0.0001	0.0012	0.0001
PEQU-E	0.2852	0.3278	ΔX	0.3000	-0.0031	0.2969	-0.0188	0.0159	-0.0055
			β_X	0.0080	0.0064	0.0144	0.0002	0.0000	-0.0000
			$[H^+]$ m.e.	0.0169	0.0144	0.0313	0.0006	-0.0076	0.0004
SP-STPS	0.2427	0.2744	ΔX	0.2540	-0.0460	0.2080	0.0063	0.0336	0.0021
			β_X	0.0070	-0.0006	0.0064	0.0002	-0.0000	-0.0000
			$[H^+]$ m.e.	0.0164	-0.0016	0.0148	0.0006	0.0021	0.0003
NA-SPSS	0.2604	0.2973	ΔX	0.2321	-0.0992	0.1329	0.0545	0.0738	0.0085
			β_X	0.0077	-0.0024	0.0053	0.0006	-0.0000	-0.0001
			$[H^+]$ m.e.	0.0185	-0.0064	0.0121	0.0030	0.0062	0.0005
NA-STSS	0.229	0.2634	ΔX	0.2281	-0.0602	0.1678	0.0172	0.0500	0.0067
			β_X	0.0059	-0.0016	0.0043	0.0005	-0.0000	-0.0000
			$[H^+]$ m.e.	0.0151	-0.0042	0.0109	0.0011	0.0045	0.0004
NA-STPS	0.2155	0.2488	ΔX	0.1870	-0.0229	0.1641	0.0064	0.0506	0.0095
			β_X	0.0048	-0.0009	0.0039	-0.0000	-0.0000	-0.0001
			$[H^+]$ m.e.	0.0137	-0.0025	0.0112	0.0000	0.0029	0.0003
AEQU	0.2187	0.2457	ΔX	0.2923	-0.0906	0.2017	-0.0143	0.0470	-0.0062
			β_X	0.0082	-0.0034	0.0048	-0.0010	-0.0000	-0.0000
			$[H^+]$ m.e.	0.0222	-0.0092	0.0129	-0.0021	0.0039	-0.0010
SA-STPS	0.2241	0.2563	ΔX	0.1496	0.0041	0.1537	0.0366	0.0316	0.0141
			β_X	0.0080	-0.0024	0.0056	-0.0006	-0.0000	0.0000
			$[H^+]$ m.e.	0.0199	-0.0060	0.0139	-0.0011	0.0030	-0.0005
IND-STPS	0.2208	0.2527	ΔX	0.2196	-0.0474	0.1723	0.0133	0.0426	0.0049
			β_X	0.0071	-0.0021	0.0051	-0.0003	-0.0000	0.0000
			$[H^+]$ m.e.	0.0191	-0.0055	0.0136	-0.0007	0.0023	-0.0004
SO-STSS	0.2654	0.303	ΔX	0.2559	-0.0500	0.2060	0.0244	0.0380	0.0050
			β_X	0.0119	-0.0019	0.0100	-0.0014	-0.0000	-0.0000
			$[H^+]$ m.e.	0.0258	-0.0041	0.0217	-0.0024	0.0021	-0.0004
SO-SPSS	0.325	0.3656	ΔX	0.3584	-0.0165	0.3419	-0.0256	0.0121	-0.0023
			β_X	0.0168	-0.0007	0.0160	-0.0031	-0.0000	-0.0000
			$[H^+]$ m.e.	0.0345	-0.0018	0.0327	-0.0058	0.0004	-0.0007

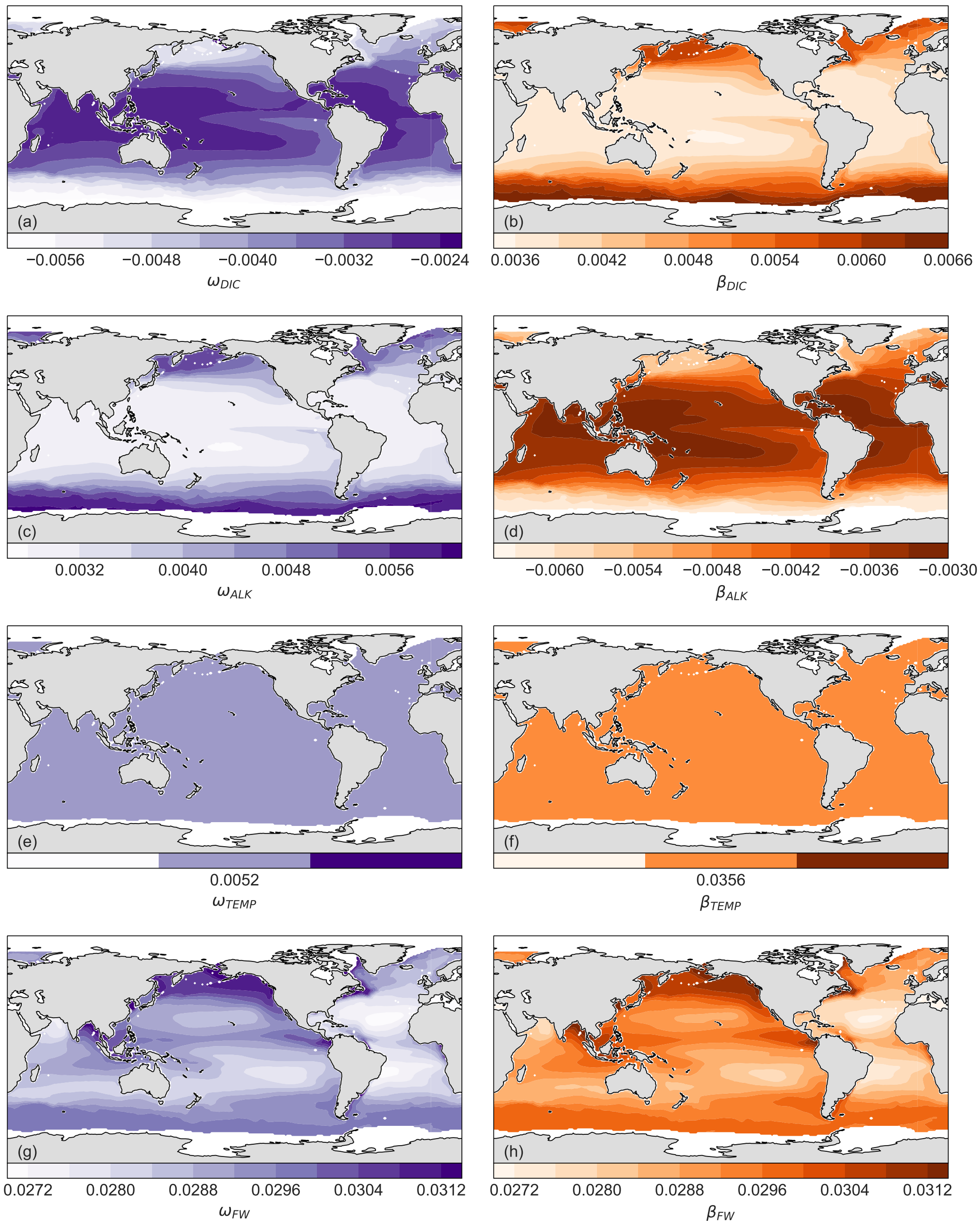

Figure S4. Maps depicting the average sensitivities of Ω (left) and $[H^+]$ (right) to changes in sDIC (a,b), sAlk (c,d), temperature (e,f), and freshwater input (g,h) in the period 1982-2020.

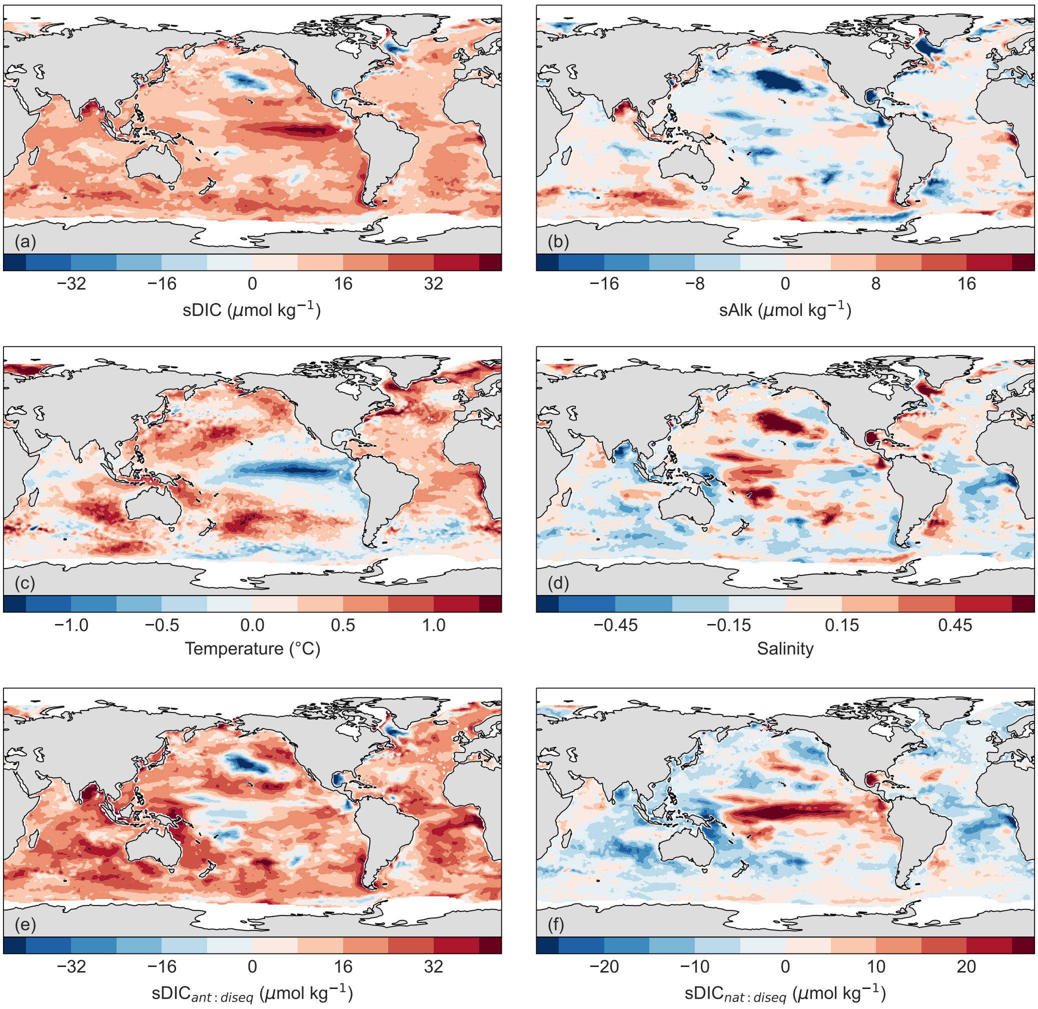

Figure S5. Maps showing the mean change (ΔX in Eq 2 and 3) in (a) sDIC, (b) sAlk, (c) temperature, (d) freshwater input, (e) sDIC$_{ant:diseq}$, and (f) sDIC$_{nat:diseq}$ from 1982 to 2021. Note that the mean change is calculated with $\Delta X = \sum_{i=1}^{N}(X_i - X_0)/N$ where X is the driver, i is the time step (years), X_0 is the first time step in X and N is the total number of years (40).

Table S5. Comparison of interannual variability among seven pCO2 products from the lowest to highest relative to OceanSODA-ETHZ: OceanSODA-ETHZ (Gregor & Gruber, 2021), CSIR-ML6 version 2019a (Gregor et al., 2019), CMEMS-FFNN (Denvil-Sommer et al., 2019), NIES-FNN (Zeng et al., 2015), MPI-SOMFFN (Landschützer et al., 2016), JMA-MLR (Iida et al., 2021), and Jena-MLS (Rödenbeck et al., 2013). Interannual variability in other data sets is scaled proportionally to that of OceanSODA-ETHZ, which is set to 1 by default.

Product	Scaled interannual variability
OceanSODA-ETHZ	1.00
CSIR-ML6 version 2019a	1.10
CMEMS-FFNN	1.31
NIES-FNN	1.56
MPI-SOMFFN	2.14
JMA-MLR	2.36
Jena-MLS	3.21

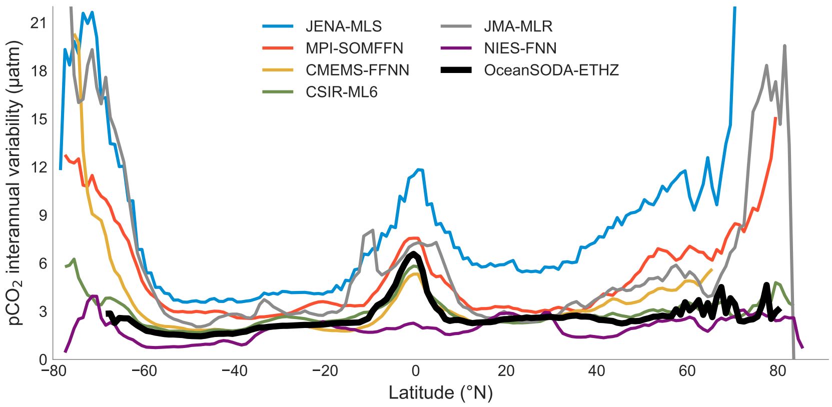

Figure S6. Comparison of zonally averaged interannual variability of pCO_2 for the seven pCO_2 products shown in Table S5.

References

Bates, N. R., Astor, Y. M., Church, M. J., Currie, K., Dore, J. E., González-Dávila, M., … Santana-Casiano, J. M. (2014). A time-series view of changing surface ocean chemistry due to ocean uptake of anthropogenic CO_2 and ocean acidification. *Oceanography*, *27*(1), 126–141.

Bates, N. R., & Johnson, R. J. (2020). Acceleration of ocean warming, salinification, deoxygenation and acidification in the surface subtropical north atlantic ocean. *Communications Earth & Environment*, *1*(1), 33.

Denvil-Sommer, A., Gehlen, M., Vrac, M., & Mejia, C. (2019). Lsce-ffnn-v1: a two-step neural network model for the reconstruction of surface ocean pco 2 over the global ocean. *Geoscientific Model Development*, *12*(5), 2091–2105.

Dore, J. E., Lukas, R., Sadler, D. W., Church, M. J., & Karl, D. M. (2009). Physical and biogeochemical modulation of ocean acidification in the central North Pacific. *Proceedings of the National Academy of Sciences*, *106*(30), 12235–12240.

Fay, A., & McKinley, G. (2014). Global open-ocean biomes: mean and temporal variability. *Earth System Science Data*, *6*(2), 273–284.

Gregor, L., & Gruber, N. (2021). OceanSODA-ETHZ: a global gridded data set of the surface ocean carbonate system for seasonal to decadal studies of ocean acidification. *Earth System Science Data*, *13*(2), 777–808.

Gregor, L., Lebehot, A. D., Kok, S., & Scheel Monteiro, P. M. (2019). A comparative assessment of the uncertainties of global surface ocean CO_2 estimates using a machine-learning ensemble (CSIR-ML6 version 2019a)–have we hit the wall? *Geoscientific Model Development*, *12*(12), 5113–5136.

Iida, Y., Takatani, Y., Kojima, A., & Ishii, M. (2021). Global trends of ocean CO_2 sink and ocean acidification: an observation-based reconstruction of surface ocean inorganic carbon variables. *Journal of Oceanography*, *77*(2), 323–358.

Landschützer, P., Gruber, N., & Bakker, D. C. (2016). Decadal variations and trends of the global ocean carbon sink. *Global Biogeochemical Cycles*, *30*(10), 1396–1417.

Ono, H., Kosugi, N., Toyama, K., Tsujino, H., Kojima, A., Enyo, K., … Ishii, M. (2019). Acceleration of Ocean Acidification in the Western North Pacific. *Geophysical Research Letters*, *46*(22), 13161–13169. doi: 10.1029/2019GL085121

Rödenbeck, C., Keeling, R. F., Bakker, D. C., Metzl, N., Olsen, A., Sabine, C., & Heimann, M. (2013). Global surface-ocean pCO_2 and sea–air CO_2 flux variability from an observation-driven ocean mixed-layer scheme. *Ocean Science*, *9*(2), 193–216.

Zeng, J., Nojiri, Y., Nakaoka, S.-i., Nakajima, H., & Shirai, T. (2015). Surface ocean CO_2 in 1990–2011 modelled using a feed-forward neural network. *Geoscience Data Journal*, *2*(1), 47–51.